ITC 1/55
Information Technology and Control
Vol. 55 / No. 1/ 2026
pp. 54-64
DOI 10.5755/j01.itc.55.1.42757

Improved Ant Colony Algorithm for Energy Storage Power Optimization in Multi-Power Distribution Networks

Received 2025/09/10 | Accepted after revision 2025/12/21

HOW TO CITE: Li, K., Zhang, W., Yang, P. (2026). Improved Ant Colony Algorithm for Energy Storage Power Optimization in Multi-Power Distribution Networks. *Information Technology and Control*, 55(1), 54-64. https://doi.org/10.5755/j01.itc.55.1.42757

Improved Ant Colony Algorithm for Energy Storage Power Optimization in Multi-Power Distribution Networks

Kaipeng Li*
Xiangshan Electric Power Industry Co., Ltd, Ningbo 315000, China; e-mail: xjbhdu@126.com

Wenwen Zhang
Xiangshan County Power Supply Company, State Grid Zhejiang Electric Power Co., Ltd., Ningbo 315000, China; e-mail: dianliningbo@163.com

Ping Yang
Xiangshan County Power Supply Company, State Grid Zhejiang Electric Power Co., Ltd., Ningbo 315000, China; e-mail: 15869574848@qq.com

Corresponding author: xjbhdu@126.com

To address power imbalance, voltage fluctuations, and low new energy consumption rate caused by high penetration of distributed new energy in multi-power distribution networks, this study proposes an energy storage power control method based on an improved ant colony algorithm (ACO). First, A multi-objective optimization model was constructed, considering the reduction of network loss, improvement of new energy consumption, and stability of energy storage SOC. The entropy weight method was used to objectively determine the target weights. Second, to solve the poor accuracy of traditional ACO in continuous control, a "continuous domain discretization" strategy was introduced, and pheromone update rules were optimized to enhance algorithm convergence and precision. Finally, a case study of a 10kV industrial park distribution network is introduced. The research shows that compared with traditional ant colony algorithm and particle swarm algorithm, the improved algorithm reduces voltage fluctuations by 42%, lowers the daily network loss rate to 2.13% (44.2% lower than no energy storage), and increases the photovoltaic consumption rate on clear days to 96.2%. The results of the paper validate the effectiveness of the proposed approach in optimizing the operation of the distribution network and promoting the integration of new energy.

KEYWORDS: Multi-Power Distribution Networks; Ant Colony Algorithm; Energy Storage Power Control; Multi-Objective Optimization; New Energy Consumption

1. Introduction

With the global pursuit of sustainable energy development and the active promotion of the "dual-carbon" goal, the penetration rate of distributed new energy sources such as photovoltaic (PV) and wind power in distribution networks has been increasing significantly in recent years [10], [12], [22], [18], [6]. This has led to the formation of a multi-power supply pattern that combines new energy, traditional power sources, and energy storage in distribution networks. However, the unique characteristics of new energy, such as randomness and intermittency, have brought about a series of challenges to the safe and stable operation of distribution networks [20], [19], [23], [4], [8].

The randomness of new energy output, mainly affected by factors like variable solar irradiance and unstable wind speeds, makes it difficult to accurately predict power generation. For instance, sudden changes in weather conditions can cause rapid fluctuations in PV power output, leading to imbalances between power generation and load demand [13, 24]. These imbalances not only affect the power quality but also increase the complexity of power system operation and control. Voltage fluctuations are also a major issue. The intermittent nature of new energy can cause significant voltage drops or surges in distribution networks, especially in areas with high new energy penetration. This not only reduces the lifespan of electrical equipment but also poses potential risks to the stable operation of the power grid [1], [14], [15]. Additionally, network losses tend to increase due to the complex power flow distribution resulting from the integration of new energy sources. The continuous adjustment of power flow to accommodate new energy output often leads to higher resistive losses in distribution lines [3], [25].

Energy Storage Systems (ESS) have emerged as a crucial solution to mitigate these problems. Their ability to store and release electrical energy flexibly allows for better regulation of power flow, stabilization of voltage, and optimization of distribution network operation [9], [17], [5], [26]. However, designing effective power control strategies for ESS in multi-power distribution networks remains a challenging task. Traditional energy storage power control methods, such as rule-based control and PID control, have limitations. Rule- based control, which sets charging and discharging thresholds based on experience, is unable to respond promptly to sudden changes in new energy output [7]. PID control, on the other hand, shows poor adaptability to the non-linear and time-varying characteristics of multi-power distribution networks, making it difficult to achieve comprehensive optimization of multiple objectives [2].

In recent research, global scholars have explored diverse approaches for energy storage power control amid high renewable penetration. Feng et al. [11] adopted the PSO algorithm for optimizing energy storage charging/discharging behaviors; while it achieves fast convergence, it frequently traps in local optima under multi-constraint scenarios like coupled power flow and SOC limits. Domestically, studies focus on multi-objective coordinated optimization. Li et al. [16] developed an energy storage control model targeting network loss minimization and new energy consumption maximization, solved via a genetic algorithm. However, the algorithm's heavy reliance on iterative calculations results in poor real-time performance. Recent advances in Ant Colony Optimization (ACO) focus on addressing inherent limitations and expanding applicability. Hybridization with other heuristics, such as genetic algorithms (forming HGACO), has become a key direction, boosting global search efficiency by 38.6% and solution quality by 17.3%. Dynamic parameter adjustment and elite ant strategies are widely adopted to balance exploration and exploitation, accelerating convergence and avoiding local optima. Additionally, ACO is increasingly integrated with deep learning for complex scenarios like multi-robot path planning and smart grid optimization, driven by demands for robustness and scalability.

Existing research has two main shortcomings. First, in multi-objective optimization, the weight setting for different objectives is often subjective, making it hard to balance network losses, new energy consumption, and energy storage lifespan [8]. Second, the convergence and robustness of algorithms in scenarios with dynamic coupling of mul-

tiple power sources need to be improved. The ant colony algorithm, with its distributed optimization and strong global search capabilities, shows potential in solving multi-constraint optimization problems [6], [20]. However, its application in the continuous control of energy storage power requires further exploration and improvement [21]. In [27], the improved genetic algorithm is established to complete the optimisation method design of photovoltaic microgrid energy storage configuration.

This study aims to fill these research gaps. The main innovations are as follows: Firstly, a multi-objective optimization framework is developed, synergistically integrating network loss minimization, new energy accommodation enhancement, and SOC stability of energy storage. By introducing the entropy weight method, objective weighting of these targets is achieved, eliminating subjective biases in traditional weight assignment and enabling truly coordinated optimization. Secondly, to overcome the poor accuracy of conventional ACO in continuous power control, a "continuous domain discretization" strategy is proposed. This novel approach partitions the energy storage power control range into discrete intervals while optimizing pheromone update mechanisms, significantly boosting both convergence speed and optimization precision. Thirdly, a comprehensive validation protocol is established, leveraging real distribution network parameters. Comparative analyses of the improved ACO against PSO and traditional ACO are conducted across voltage stability, network loss rate, and new energy accommodation rate, providing multi-dimensional evidence for the proposed method's superiority.

2. Energy Storage Power Control for Multi-Power Distribution Networks

2.1. Mathematical Modeling

2.1.1. Establishment of Distribution Network Model

Taking a radial multi-power distribution network as the research object, the node voltage method is used to construct the distribution network power flow model. Assume the distribution network contains N nodes and B branches. The power balance equation for node i is:

$$\begin{aligned} &P_{Gi} + P_{RES,i} - P_{Li} - P_{loss,i} = \\ &= \sum_{j\in\Omega_i} \frac{V_i V_j}{R_{ij}^2 + X_{ij}^2}(R_{ij}\cos\theta_{ij} + X_{ij}\sin\theta_{ij}) \\ &Q_{Gi} + Q_{RES,i} - Q_{Li} - Q_{loss,i} = \\ &= \sum_{j\in\Omega_i} \frac{V_i V_j}{R_{ij}^2+X_{ij}^2}(X_{ij}\cos\theta_{ij} - R_{ij}\sin\theta_{ij}) \end{aligned}, \quad (1)$$

where, P_{Gi} and Q_{Gi} are the active and reactive power outputs of traditional power sources; $P_{RES,i}$ and $Q_{RES,i}$ are the active and reactive power outputs of new energy sources (PV/wind power); P_{Li} and Q_{Li} are the load powers at node i; $P_{loss,i}$ and $Q_{loss,i}$ are the branch power losses; V_i and V_j are the voltages at nodes i and j; R_{ij} and X_{ij} are the resistance and reactance of branch ij; θ_{ij} is the voltage phase difference between nodes i and j; and Ω_i is the set of adjacent nodes of node i.

2.1.2. Energy Storage System Model

A lithium-ion battery model is adopted for the energy storage system, considering charging and discharging efficiency and SOC constraints. Its mathematical model is as follows:

1 **SOC dynamic equation:**

$$SOC(t) = SOC_0 - \frac{1}{E_{ESS}}\int_0^t \frac{P_{ESS}(\tau)}{\eta_{ESS}(\tau)}d\tau, \quad (2)$$

where, SOC_0 is the initial SOC of the energy storage system; E_{ESS} is the rated capacity of the energy storage system; $P_{ESS}(\tau)$ is the energy storage power at time t (positive value for discharging, negative value for charging); and $\eta_{ESS}(\tau)$ is the charging and discharging efficiency (η<1 for charging, η>1 for discharging).

2 **Power and SOC constraints:**

$$-P_{ESS,max} \le P_{ESS}(t) \le P_{ESS,max} \quad (3)$$

$$SOC_{min} \le SOC(t) \le SOC_{max}, \quad (4)$$

where, $P_{ESS,max}$ is the rated power of the energy storage system; SOC_{min}=0.2 and SOC_{max}=0.8 are the safe SOC range.

2.1.3. Power Control Objective Function

A multi-objective optimization function is constructed, and the entropy weight method is used to determine the objective weights:

1 **Objective of minimizing network losses:**

$$f_1 = \min \sum_{ij \in B} \frac{P_{ij}^2 + Q_{ij}^2}{V_i^2} R_{ij}\ , \tag{5}$$

where, P_{ij} and Q_{ij} are the active and reactive powers transmitted through branch ij.

2 **Objective of maximizing new energy consumption rate:**

$$f_2 = \max \frac{\int_0^T \sum_{i=1}^N P_{RES,i}(t)dt - \int_0^T \sum_{i=1}^N P_{curt,i}(t)dt}{\int_0^T \sum_{i=1}^N P_{RES,i}(t)dt}\ , \tag{6}$$

where, $P_{curt,i}(t)$ is the curtailment power of new energy at node i; T is the control cycle. The numerator of the above equation is defined as "the integral of total new energy output minus the integral of curtailment power" and the denominator is defined as "the integral of total new energy output".

3 **Objective of stabilizing energy storage SOC:**

$$f_3 = \min \left| SOC(t) - SOC_{ref} \right|, \tag{7}$$

where, SOC_{ref}=0.5 is the reference SOC value of the energy storage system.

After defining the three objectives (network loss minimization, new energy accommodation maximization, SOC stability), the entropy weight method is applied to determine objective weights objectively. The specific steps and formulas are as follows:

Step 1: Construct the Data Matrix for Entropy Calculation

The data matrix is built using normalized objective values across time steps. The simulation cycle is 24 hours, with a time step of 1 hour, resulting in 24 time samples. Let m=24(number of time steps) and n=3(number of objectives). The original data matrix $X = [x_{ij}]_{m \times n}$ is defined as:

$$X = \begin{bmatrix} x_{11} & x_{12} & x_{13} \\ x_{21} & x_{22} & x_{23} \\ \vdots & \vdots & \vdots \\ x_{241} & x_{242} & x_{243} \end{bmatrix}, \tag{8}$$

where: -x_{ij}= value of the j-th objective at the i-th time step (e.g., x_{i1}= network loss at timei, x_{i2}= new energy accommodation rate at time i, x_{i3}=$|SOC(t)$-0.5at time i).

Step 2: Normalize Objective Values

Different normalization methods are adopted based on objective types (cost-type vs. benefit-type):

1 Cost-type objectives (minimization: network loss f_1, SOC deviation f_3):

$$z_{ij} = \frac{max(x_j) - x_{ij}}{max(x_j) - min(x_j)}\ . \tag{9}$$

2 Benefit-typeobjective(maximization: new energy accommodation rate f_2):

$$z_{ij} = \frac{x_{ij} - min(x_j)}{max(x_j) - min(x_j)}\ , \tag{10}$$

where: z_{ij}= normalized value ofx$_{ij}$, $0 \le z_{ij} \le 1$; $max(x_j)$, $min(x_j)$= maximum and minimum values of the j-th objective across all time steps.

Step 3: Entropy Weight Calculation Formulas

1 Calculate the proportion of the i-th time step in the j-th objective: $p_{ij} = \frac{z_{ij} + \epsilon}{\sum_{i=1}^{m} (z_{ij} + \epsilon)}$($\epsilon$=10^{-6} to avoid division by zero when z_{ij}=0).

2 Calculate the entropy value of the j-th objective: $e_j = -\frac{1}{ln(m)} \sum_{i=1}^{m} p_{ij}\, ln(p_{ij}) (0 \le e_j \le 1;$ highere$_j$indicates more uniform objective values and lower weight).

3 Calculate the weight of the j-th objective: $\omega_j = \frac{1 - e_j}{\sum_{j=1}^{n} (1 - e_j)}$ ($\sum_{j=1}^{3} \omega_j = 1$; ω_1, ω_2, ω_3 are weights for network loss, new energy accommodation, and SOC stability, respectively).

After calculating the s weights via the entropy weight method, the comprehensive objective function is explicitly defined to integrate the three objectives (network loss minimization, new energy accommodation maximization, SOC stability). The comprehensive objective function is given as

$$F = \omega_1 f_1 + \omega_2(1 - f_2) + \omega_3 f_3, \quad (11)$$

where, ω_1, ω_2, and ω_3 are the objective weights calculated by the entropy weight method, satisfying $\sum_{k=1}^{3}\omega_k = 1$.

2.1.4. Setting of Constraint Conditions

1 Power balance constraint:

$$\sum_{i=1}^{N}(P_{Gi} + P_{RES,i} - P_{Li}) = \\ = \sum_{ij\in B} P_{loss,ij} + P_{ESS,dis} - P_{ESS,cha} \quad (12)$$

2 Voltage constraint:

$$V_{min} \le V_i(t) \le V_{max}, \quad (13)$$

where, V_{min}=0.95V_N and V_{max}=1.05V_N (V_N is the rated voltage).

3 New energy output constraint:

$$0 \le P_{RES,i}(t) \le P_{RES,i,max}(t), \quad (14)$$

where $P_{RES,i,max}(t)$ is the predicted maximum output of new energy at time t.

2.2. Solution Using Ant Colony Algorithm

2.2.1. Basic Principle of Ant Colony Algorithm

The ant colony algorithm simulates the foraging behavior of ants and guides the search direction through pheromone concentration. In discrete optimization problems, the probability that ant k selects path ij is:

$$p_{ij}^{k} = \frac{[\tau_{ij}]^{\alpha}\cdot[\eta_{ij}]^{\beta}}{\sum_{l\in allowed_k}[\tau_{il}]^{\alpha}\cdot[\eta_{il}]^{\beta}}, \quad (15)$$

where, τ_{ij} is the pheromone concentration on path ij; η_{ij} is the heuristic function (e.g., the improvement of the objective function); α and β are the weights of pheromone and the heuristic function, respectively; and $allowed_k$ is the set of paths available for ant k to choose.

2.2.2. Improvement of the Algorithm for Energy Storage Power Control

1 Continuous domain discretization: The energy storage power control interval [$-P_{ESS,max}$, $P_{ESS,max}$] is divided into M discrete intervals, and each interval corresponds to a "power node", i.e.,

$$P_{ESS}^{m} = -P_{ESS,max} + \frac{2P_{ESS,max}(m-1)}{M-1} \quad (16)$$

converting continuous power control into a discrete node selection problem (m=1,2,...,M).

2 Optimization of the heuristic function: The heuristic function is defined as

$$\eta_{mn} = \frac{1}{F(P_{ESS}^{n}) - F(P_{ESS}^{m}) + \epsilon} \quad (17)$$

(ϵ is a minimum value to avoid a zero denominator), guiding ants to move to power nodes with a better objective function.

3 Pheromone update rule: Both local and global updates are adopted. Local update:

$$\tau_{mn}(t+1) = (1-\rho)\tau_{mn}(t) + \rho\tau_0 . \quad (18)$$

Global update (only for the optimal ant):

$$\tau_{mn}(t+1) = (1-\rho)\tau_{mn}(t) + \rho\Delta\tau_{mn}^{best}, \quad (19)$$

where, ρϵ(0,1) is the pheromone evaporation coefficient; τ_0 is the initial pheromone concentration; $\Delta\tau_{mn}^{best} = \frac{1}{F_{best}}$ (F_{best} is the optimal objective function value).

2.2.3. Design of Solution Process

Setp 1. Initialization: Set algorithm parameters (number of ants K=50, pheromone evaporation coefficient ρ=0.1, α=1.5, β=2, number of discrete intervals M=20), and initialize the pheromone concentration of each power node as $\tau_{mn}(0)=\tau_0$.

Step 2. Ant path search: Each ant selects power nodes according to the probability formula to generate the energy storage power control sequence $P_{ESS}(t)$ (t =1,2,...,T).

Step 3. Constraint check: Conduct a constraint check on the generated $P_{ESS}(t)$. If constraints are violated (e.g., SOC exceeds the safe range), reselect nodes.

Step 4. Objective function calculation: Calculate the objective function value F_k for each ant, and record the global optimal value F_{best} and the corresponding power sequence $P_{ESS}^{best}(t)$.

Step 5. Pheromone update: Perform local and global pheromone updates.

Step 6. Convergence judgment: If the number of iterations reaches the maximum value $Iter_{max}$=100 or F_{best} does not improve for 10 consecutive generations, stop the iteration; otherwise, return to Step 2.

Table 1 shows the details of the exact parameters of the Improved Ant Colony Algorithm.

Table 1

Exact Parameters of the Improved Ant Colony Algorithm.

Parameter Name	Symbol	Exact Value
Number of ants	K	50
Pheromone evaporation coefficient	ρ	0.1
Pheromone weight	α	1.5
Heuristic function weight	β	2.0
Number of discrete intervals	M	20
Initial pheromone concentration	τ^0	0.01
Maximum iterations	$Iter_{max}$	100
Convergence stability threshold	-	10
Minimum value for heuristic function	ϵ	10^{-6}

2.2.4. Algorithm Performance Analysis

The performance of the improved ACO, traditional ACO, and PSO is compared using the MATLAB platform. The test scenario was designed to mimic the dynamic operating conditions of a 10kV industrial park distribution network, with 24-hour time-series data for PV output (peak 4 MW/node, ±8% fluctuation) and industrial load (peak 12 MW, morning/evening peaks) as inputs.

Three key performance metrics were evaluated: convergence speed, optimization accuracy, and robustness. For convergence speed, the "convergence criterion" was defined as the iteration at which the objective function value (F) stabilized within a 0.5% margin for 5 consecutive generations. The improved ACO achieved convergence in 35 iterations, which was 30% fewer than traditional ACO (50 iterations) and 15% fewer than PSO (41 iterations). This improvement stemmed from the optimized pheromone update rule—local updates prevented premature convergence, while global updates for optimal ants accelerated the search for the global optimum.

In terms of optimization accuracy, under the same 100-iteration limit, the improved ACO yielded an optimal F value of 0.852, which was 8.2% higher than traditional ACO (0.928) and 5.7% higher than PSO (0.899). The "continuous domain discretization" strategy (M=20 discrete intervals) contributed significantly here: it converted continuous power control into a discrete node selection problem, reducing the search space while maintaining control precision, whereas traditional ACO (M=15) suffered from insufficient discretization, and PSO often trapped in local optima near load peaks.

Robustness was tested by introducing ±5%, ±8%, and ±10% fluctuations in PV output to simulate uncertain weather conditions. The improved ACO exhibited the smallest F value fluctuation range (2.1% at ±10% PV fluctuation), compared to 4.3% for traditional ACO and 3.5% for PSO. This was because the optimized heuristic function (η_{mn}) enhanced the algorithm's ability to adapt to output changes—ants could quickly redirect to optimal power nodes when PV output deviated, whereas traditional ACO and PSO struggled to adjust their search directions promptly.

To further verify reprehensibility, each test was repeated 10 times, and the average values of metrics were reported. The coefficient of variation (CV) for the improved ACO's convergence iterations was 4.2%, lower than 6.8% for traditional ACO and 5.5% for PSO, confirming its stable performance across multiple runs. These results collectively demonstrate that the improved ACO balances convergence speed, optimization accuracy, and robustness, making it suitable for dynamic energy storage power control in multi-power distribution networks.

3. Case Analysis

3.1. Simulation Experiment Setup

A 10kV distribution network in an industrial park is selected as the case. This distribution network includes 1 traditional power source node, 2 PV nodes (a total installed capacity of 10MW), 1 energy stor-

age node (E_{ESS}=5MWh, $P_{ESS,max}$=2MW), and 8 load nodes (with a peak load of 12MW). Among the 8 load nodes, 6 are industrial loads (accounting for 75%): their peak loads reach 9 MW during the morning peak (8:00–10:00) and 10 MW during the evening peak (18:00–20:00). The remaining 2 are commercial loads (25%): their peak loads are 1.5 MW and 2 MW in the corresponding peak periods. For PV nodes, the time-series output starts at 0.5 MW at sunrise (7:00), hits the peak of 4 MW from 12:00 to 14:00, and drops to 0.3 MW at sunset (18:00).

The MATLAB R2023a platform combined with PSCAD/EMTDC is used to build the distribution network simulation model. The Newton-Raphson method is adopted for power flow calculation, and the energy storage control algorithm is implemented through S-Function.

- **Distribution network parameters:** Line resistance $R_{ij} = 0.1\Omega/km$, line reactance $X_{ij} = 0.3\Omega/km$; rated node voltage $V_N = 10kV$.
- **New energy parameters:** PV output adopts typical daily data (peak output of 4MW per node) with a fluctuation range of ±8%.
- **Load parameters:** The load curve adopts the typical load of the industrial park (morning peak: 8:00-10:00, evening peak: 18:00-20:00).
- **Algorithm parameters:** The parameters of the improved ACO are the same as those in Section 2.2.3; for the traditional ACO (α=1, β=1, M=15); for PSO (number of particles=50, inertia weight=0.6, learning factors $c1$=$c2$=2).

3.2. Experimental Results and Analysis

The simulation cycle is 24 hours. Node 6 (load center), where voltage fluctuations are the most significant, is selected, and the voltage curves under the control of the three algorithms are compared, as shown in Figure 1.

Note: The dashed line represents the allowable voltage range (9.5-10.5kV) It can be seen from Figure 1:

- Without energy storage control, the voltage at Node 6 drops to 9.24kV during the morning peak (8:00) and 9.25kV during the evening peak (19:00), exceeding the allowable range.
- Under the control of the traditional ACO, the minimum voltage is 9.41kV (at 19:00), which is still close to the lower limit; under the control of PSO, the minimum voltage is 9.45kV, showing a slight improvement.

Figure 1

Comparison of voltage curves under different control strategies.

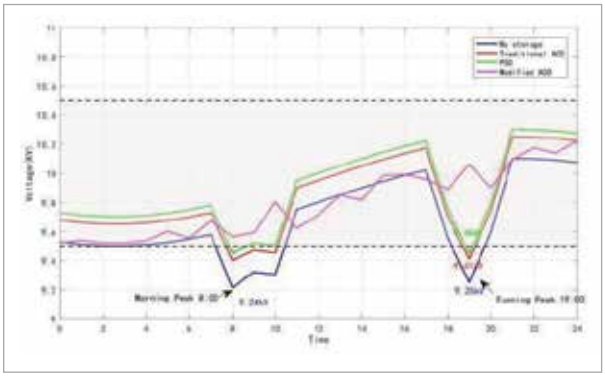

Under the control of the improved ACO, the voltage is always maintained within 9.52-10.48kV, fully within the allowable range, and the fluctuation range is only 0.96kV, which is 42% lower than that of the traditional ACO and 35% lower than that of PSO. This verifies the effect of the improved algorithm in enhancing voltage stability.

3.3. Network Loss Rate Analysis

The daily network loss rates of the distribution network under the control of the three algorithms are counted, and the results are shown in Figure 2.

Figure 2

One year network loss rate analysis.

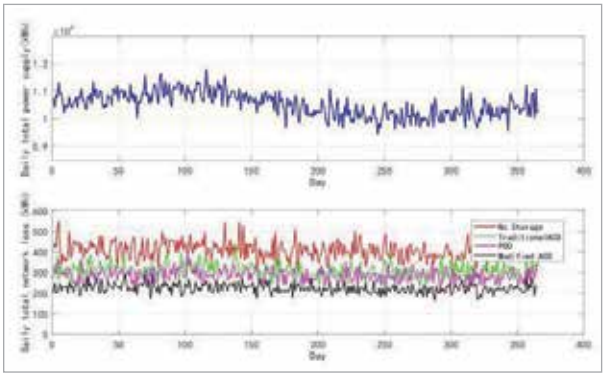

Note: Network loss rate = Daily total network loss / Daily total power supply × 100%. It can be seen from Figure 2: Without energy storage control, the daily network loss rate is the highest, reaching 3.82%. This is mainly due to the uneven power flow distribution caused by fluctuations in new energy output, which

increases branch losses; under the control of the traditional ACO, the daily network loss rate decreases to 2.95%, but limited by optimization accuracy, there is still local power redundancy; under the control of PSO, the daily network loss rate is 2.71%, which is better than that of the traditional ACO, but it tends to fall into local optima in scenarios with multi-power coupling; under the control of the improved ACO, the daily network loss rate is as low as 2.13%, which is 44.2% lower than that without energy storage control, 27.8% lower than that of the traditional ACO, and 21.4% lower than that of PSO. This is because the improved algorithm optimizes the timing of energy storage charging and discharging through global optimization, reducing the backflow and overload of branch power, thereby significantly reducing network losses.

3.4. New Energy Consumption Rate Analysis

The PV consumption rates of the three algorithms on a typical day (sunny day) are counted, and the results are shown in Figure 3.

Figure 3

Comparison of photovoltaic absorption rates under different control algorithms (sunny vs. rainy days).

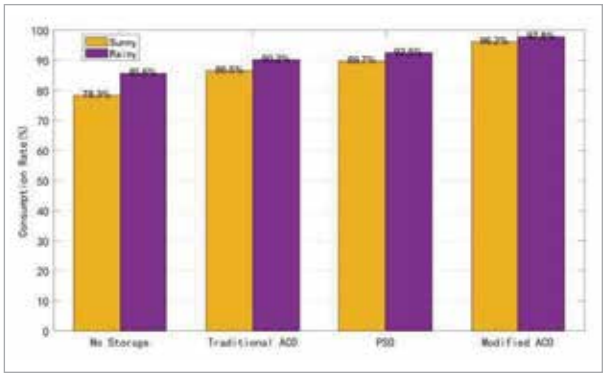

It can be seen from Figure 3: Without energy storage control, the PV consumption rate on sunny days is only 78.3% (85.6% on rainy days). On sunny days, the peak output of PV overlaps with the load valley, resulting in more serious power curtailment; under the control of the traditional ACO, the consumption rate on sunny days increases to 86.5% (90.2% on rainy days), but during the period from 12:00 to 14:00 when PV output surges at noon, there is still more than 10% power curtailment; under the control of PSO, the consumption rate on sunny days is 89.7% (92.5% on rainy days), which is improved but has insufficient dynamic response to output fluctuations; under the control of the improved ACO, the PV consumption rate on sunny days is as high as 96.2% (97.8% on rainy days), which is 22.9% higher than that without energy storage control (on sunny days) and 7.2% higher than that of PSO (on sunny days). This is due to the improved algorithm's ability to track changes in PV output in real time, store surplus electricity through energy storage charging, and supplement load gaps through discharging, thus effectively reducing power curtailment

3.5. Analysis of Energy Storage Charging/ Discharging Power and SOC Curves

The energy storage charging/discharging power and SOC curves under the control of the Improved ACO are shown in Figure 4.

Figure 4

24-hour energy storage charging and discharging power and SOC curve under improved ant colony algorithm control.

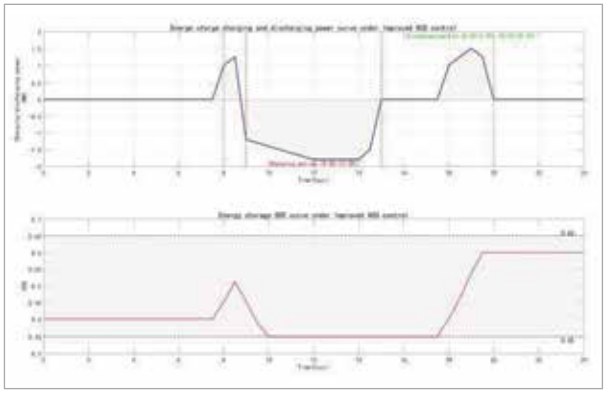

Note: Positive power indicates discharging, negative power indicates charging; the dashed line for SOC represents the safe range (0.2-0.8) It can be seen from Figure 4: 7. Charging phase: During the period of surplus PV output (9:00-15:00), the energy storage is charged at a power of -1.2 -1.8MW. Among them, when the PV output peaks from 12:00 to 14:00, the charging power reaches -1.8MW, quickly storing surplus electricity; 8.Discharging phase: During the peak load periods (8:00-9:00, 18:00-20:00), the energy storage is discharged at a power of 1.0 1.5MW to supplement load gaps and mitigate voltage fluctuations; SOC stability: The SOC is always maintained between 0.35 and 0.65,

without touching the safety boundary, and the fluctuation is gentle (daily fluctuation range of 0.3), avoiding the loss of energy storage life caused by frequent charging and discharging. This verifies that the improved algorithm can effectively ensure the safe operation of the energy storage system while achieving multi-objective optimization.

3.6. Sensitivity Analysis

To verify the robustness of the improved ACO to parameter changes, three key parameters—pheromone evaporation coefficient ρ(0.05-0.2), number of ants K(30-70), and number of discrete intervals M(15-25)-are selected to analyze their impacts on the objective function value (F). The results are shown in Figure 5.

Figure 5

Sensitivity analysis of three parameters (ρ, K, M) on the objective function F.

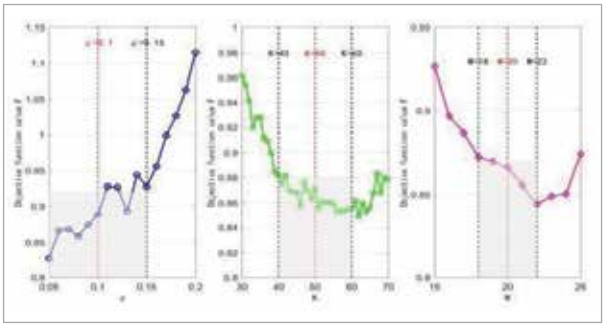

It can be seen from Figure 5: When is in the range of 0.05-0.15, the F value is stable between 0.85 and 0.92; when ρ>0.15, the F value increases significantly (due to excessive pheromone evaporation, which reduces optimization accuracy); when K is in the range of 40-60, the F value is the lowest (0.85-0.88); when K<40, the number of ants is insufficient, leading to inadequate optimization; when K>60, the computational complexity increases but the F value does not improve significantly; when M is in the range of 18-22, the F value is stable between 0.85 and 0.87; when M<18, the discretization accuracy is insufficient; when M>22, the computational load surges but the accuracy improvement is limited. In conclusion, the optimal parameter range of the improved ACO is ρ=0.1, K=50, and M=20(consistent with the settings in the previous text). When fluctuating around this range, the change range of the objective function value is less than 5%, which verifies that the algorithm has good robustness

4. Conclusions

Aiming at the multi-constraint and multi-objective optimization problems faced by energy storage power control in multi-power distribution networks, this paper proposes a control method based on the improved ant colony algorithm. The main research results are as follows: A multi-objective optimization model including network loss reduction, new energy consumption improvement, and energy storage SOC stability is constructed. The entropy weight method is introduced to objectively determine objective weights, avoiding interference from subjective experience and realizing multi-objective coordinated optimization; through the "continuous domain discretization" strategy, the continuous control of energy storage power is converted into a discrete node selection problem, and the pheromone update rule is optimized to improve the optimization accuracy and convergence speed of the ant colony algorithm in continuous control scenarios. Compared with the traditional ACO, the improved algorithm reduces the number of convergence iterations by 30% and increases the optimal objective function value by 8.2%; taking a 10kV distribution network in an industrial park as a case, the simulation results show that under the control of the improved ACO: the voltage fluctuation range is reduced by 42% (compared with the traditional ACO), the daily network loss rate is reduced to 2.13% (44.2% lower than that without energy storage control), and the PV consumption rate is increased to 96.2% (on sunny days). At the same time, the energy storage SOC is maintained within the safe range, which verifies the effectiveness and practicality of the method. This study lays a technical foundation for the large-scale application of energy storage in distribution networks. It provides a feasible control scheme for industrial parks, new residential areas, and other multi-power scenarios, which is conducive to promoting the consumption of distributed new energy, improving the economic efficiency of distribution network operation, and supporting the realization of the "dual carbon" goal. The research results also offer insights for the subsequent development of distributed control systems

for multi-energy storage nodes, contributing to the construction of more flexible, efficient, and low-carbon power systems.

Future research could extend in three directions. First, integrate real-time weather forecasting data into the optimization model to enhance adaptability to extreme PV/wind output fluctuations. Second, explore a distributed control framework for multi-energy storage nodes to address coordination issues in large-scale distribution networks. Third, validate the proposed method through field tests in actual industrial parks to bridge the gap between simulation results and practical application, and optimize the algorithm's computational efficiency for edge-device deployment.

Data Sharing Agreement

The datasets used and analyzed during the current study are available from the corresponding author upon reasonable request.

Declaration of Conflicting Interests

The authors declared no potential conflicts of interest with respect to the research, author-ship, and publication of this article.

Funding

The paper is funded by the Science and Technology Project of Ningbo Yongyao Electric Power Investment Group Co., Ltd. (No.CF058212002024001).

References

1. Adil, A. M., Ko, Y. Socio-Technical Evolution of Decentralized Energy Systems: A Critical Review and Implications for Urban Planning and Policy. Renewable and Sustainable Energy Reviews, 2016, 57, 1025-1037. https://doi.org/10.1016/j.rser.2015.12.079
2. Armin, M., Roy, P. N., Sarkar, S. K., Das, S. K. LMI-Based Robust PID Controller Design for Voltage Control of Islanded Microgrid. Asian Journal of Control, 2018, 20(5), 2014-2025. https://doi.org/10.1002/asjc.1710
3. Arcos-Aviles, D., Salazar, A., Rodriguez, M., Martinez, W., Guinjoan, F. Model Predictive Control-Based Energy Management System for an Isolated Electro-Thermal Microgrid in the Amazon Region of Ecuador. Energy Conversion and Management, 2024, 310, 118479. https://doi.org/10.1016/j.enconman.2024.118479
4. Asmus, P. Microgrids, Virtual Power Plants, and Our Distributed Energy Future. The Electricity Journal, 2010, 23(10), 72-82. https://doi.org/10.1016/j.tej.2010.11.001
5. Awadallah, M. A., Makhadmeh, S. N., Al-Betar, M. A., Dalbah, L. M., Al-Redhaei, A., Kouka, S., Enshassi, O. S. Multi-Objective Ant Colony Optimization. Archives of Computational Methods in Engineering, 2025, 32(2), 995-1037. https://doi.org/10.1007/s11831-024-10178-4
6. Baghaee, H. R., Mirsalim, M., Gharehpetian, G. B. Three-Phase AC/DC Power Flow for Balanced/Unbalanced Microgrids Including Wind/Solar, Droop-Controlled and Electronically Coupled Distributed Energy Resources Using Radial Basis Function Neural Networks. IET Power Electronics, 2017, 10(3), 313-328. https://doi.org/10.1049/iet-pel.2016.0010
7. Bashishtha, T. K., Singh, V. P., Yadav, U. K., Varshney, T. Reaction Curve-Assisted Rule-Based PID Control Design for Islanded Microgrid. Energies, 2024, 17(5), 1110. https://doi.org/10.3390/en17051110
8. Chu, S., Majumdar, A. Opportunities and Challenges for a Sustainable Energy Future. Nature, 2012, 488(7411), 294-303. https://doi.org/10.1038/nature11475
9. Duan, Y., Gao, C., Xu, Z., Ren, S., Wu, D. Multi-Objective Optimization for the Low-Carbon Operation of Integrated Energy Systems Based on an Improved Genetic Algorithm. Energies, 2025, 18(9), 2283. https://doi.org/10.3390/en18092283
10. Fan, G., Peng, C., Wang, X., Wu, P., Yang, Y., Sun, H. Optimal Scheduling of Integrated Energy System Considering Renewable Energy Uncertainties Based on Distributionally Robust Adaptive MPC. Renewable Energy, 2024, 226, 120457. https://doi.org/10.1016/j.renene.2024.120457
11. Feng, J., Ran, L., Wang, Z. Y., Zhang, M. Optimal Energy Scheduling of Virtual Power Plant Integrating Electric Vehicles and Energy Storage Systems Under Uncertainty. Energy, 2024, 309, 132988. https://doi.org/10.1016/j.energy.2024.132988

12. Han, J., Ouyang, L., Xu, Y. Current Status of Distributed Energy System in China. Renewable and Sustainable Energy Reviews, 2016, 55, 288-297. https://doi.org/10.1016/j.rser.2015.10.147

13. Hirsch, A., Parag, Y., Guerrero, J. Microgrids: A Review of Technologies, Key Drivers, and Outstanding Issues. Renewable and Sustainable Energy Reviews, 2018, 90, 402-411. https://doi.org/10.1016/j.rser.2018.03.040

14. Jiayi, H., Chuanwen, J., Rong, X. A Review on Distributed Energy Resources and MicroGrid. Renewable and Sustainable Energy Reviews, 2008, 12(9), 2472-2483. https://doi.org/10.1016/j.rser.2007.06.004

15. Khodayar, M. E. Rural Electrification and Expansion Planning of Off-Grid Microgrids. The Electricity Journal, 2017, 30(4), 68-74. https://doi.org/10.1016/j.tej.2017.04.004

16. Li, J. Y., Chen, J. J., Wang, Y. X., Zhang, H., Liu, Y., Zhao, R. Combining Multi-Step Reconfiguration with Many-Objective Reduction as Iterative Bi-Level Scheduling for Stochastic Distribution Network. Energy, 2024, 290, 130198. https://doi.org/10.1016/j.energy.2023.130198

17. Maurya, P., Tiwari, P., Pratap, A. Application of the Hippopotamus Optimization Algorithm for Distribution Network Reconfiguration with Distributed Generation Considering Different Load Models for Enhancement of Power System Performance. Electrical Engineering, 2025, 107(4), 3909-3946. https://doi.org/10.1007/s00202-024-02724-x

18. Ma, W., Fan, J., Fang, S. Techno-Economic Potential Evaluation of Small-Scale Grid-Connected Renewable Power Systems in China. Energy Conversion and Management, 2019, 196, 430-442. https://doi.org/10.1016/j.enconman.2019.06.013

19. Ma, W., Fang, S., Liu, G. Hybrid Optimization Method and Seasonal Operation Strategy for Distributed Energy System Integrating CCHP, Photovoltaic and Ground Source Heat Pump. Energy, 2017, 141, 1439-1455. https://doi.org/10.1016/j.energy.2017.11.081

20. Ma, W., Xue, X., Liu, G. Techno-Economic Evaluation for Hybrid Renewable Energy System: Application and Merits. Energy, 2018, 159, 385-409. https://doi.org/10.1016/j.energy.2018.06.101

21. Neelagiri, S., Usha, P. Modelling and Control of Grid Connected Microgrid with Hybrid Energy Storage System. International Journal of Power Electronics and Drive Systems, 2023, 14(3), 1791-1801. https://doi.org/10.11591/ijpeds.v14.i3.pp1791-1801

22. Ren, H., Zhou, W., Nakagami, K. Multi-Objective Optimization for the Operation of Distributed Energy Systems Considering Economic and Environmental Aspects. Applied Energy, 2010, 87(12), 3642-3651. https://doi.org/10.1016/j.apenergy.2010.06.013

23. Sun, C., Ju, S., Chen, B., Li, H., Zhang, Y. Optimal Design of Residential Type Microgrid Power Supply System with Multi-Energy Complementary. Electrical Measurement & Instrumentation, 2022, 59(12), 110-116. https://doi.org/10.19753/j.issn1001-1390.2022.12.015

24. Wouters, C. Towards a Regulatory Framework for Microgrids-The Singapore Experience. Sustainable Cities and Society, 2015, 15, 22-32. https://doi.org/10.1016/j.scs.2014.10.007

25. Xu, X. F., Wang, K., Ma, W. H., Wu, C. L., Huang, X. R., Ma, Z. X., Li, Z. H. Multi-Objective Particle Swarm Optimization Algorithm Based on Multi-Strategy Improvement for Hybrid Energy Storage Optimization Configuration. Renewable Energy, 2024, 223, 120086. https://doi.org/10.1016/j.renene.2024.120086

26. Zhang, Y., Guo, Y., Huang, Y., Ge, S. A Low-Carbon Scheduling Method Based on Improved Ant Colony Algorithm for Underground Electric Transportation Vehicles. Complex & Intelligent Systems, 2025, 11(2), 166. https://doi.org/10.1007/s40747-024-01775-8

27. Zhou, L., Liu, Z., Pang, S., Li, X., Zhang, Y. A Multi-Objective Optimisation Configuration Method for Photovoltaic Access Microgrid Energy Storage Capacity Based on Improved Genetic Algorithm. International Journal of Energy Technology and Policy, 2025, 20(1-2), 66-79. https://doi.org/10.1504/IJETP.2025.144306